



# Model Prediction Control with Common Mode Voltage Suppression for Dual Three-Phase PMSM

Congqi Feng, Wu Liao<sup>✉</sup>, Sheng Huang, Zexing Chen, Ge Liang, and Yu Liu

College of Electrical and Information Engineering, Hunan University, Lushan Road (S), Yuelu District, Changsha, Hunan, China  
liaowu1988@hnu.edu.cn

**Abstract.** The system composed of dual three-phase permanent magnet synchronous motor and PWM inverter has high common mode voltage (CMV). Aiming at these problems, this article analyzed the common mode voltage characteristics of the six-phase voltage space vector and proposed a model predictive current control method (SCMV-MPCC) to suppress common mode voltage. The virtual voltage vectors ( $V^3_s$ ) that suppress common-mode voltage were structured by linearly combining the four adjacent large vectors from 64 basic vectors, which become zero vectors in the  $z_1z_2$  planes to suppress the harmonic current. Therefore, the CMV term and  $z_1z_2$  plane harmonic current term in the cost function can be ignored. This method avoided the adjustment of multiple weight factors and optimized the prediction model. In the MPCC method, by synthesizing the low common mode voltage zero vector and introducing the duty cycle control, the optimal configuration of the action time of the virtual vector and the synthetic zero vector is realized, to reduce the stator current ripple. This method can limit the CMV to  $\pm V_{dc}/6$  and the peak-to-peak value of CMV is one third of converter DC-bus voltage under such condition as the harmonic current of stator winding is effectively restrained. Simulation results show that the proposed SCMV-MPCC method is correct and effective.

**Keywords:** Dual three-phase · Suppression of common-mode voltage (CMV) · Virtual voltage vectors · Model predictive control · Duty cycle

## 1 Introduction

Dual three-phase permanent magnet synchronous motors (PMSM) cross-fuse the advantages of multi-phase motors and permanent magnet motors, such as small torque ripple, strong fault tolerance, etc., and have received extensive attention in the fields of wind power generation and electric drive [1]. Model Predictive Control (MPC), as a control method with simple and intuitive concept, easy to model and without complicated parameter design, has been widely used in motor drives, power electronic converters and other fields in recent years. At present, the research of MPC method in the field of

motor drive mainly focuses on the finite control set MPC (FCS-MPC), which has fast dynamic response and can perform multi-objective control.

The AC motor speed control system generally uses pulse width modulation technology, and there will be a common-mode voltage (CMV) between the node of the stator winding and the midpoint of the inverter. Take the double Y-shifted  $30^\circ$  dual three-phase PMSM in which the star nodes of the stator windings are isolated from each other. The composed system will produce a larger common-mode voltage, which can be represented by the voltage between the star node of the stator winding and the midpoint of the DC bus of the converter. The common-mode voltage will bring adverse effects such as winding insulation degradation, electromagnetic interference, and common-mode current to the system, so it is necessary to suppress the common-mode voltage. Usually common-mode voltage suppression methods focus on the following aspects: motor structure, converter structure, modulation algorithm and filter, etc. [2-4].

For dual three-phase PMSM, the current FCS-MPC method mainly focuses on indicators such as motor current, torque, and speed. There are few studies on how to effectively suppress the common-mode voltage of dual-three-phase PMSM while achieving these performance indicators. The common-mode voltage suppression method for dual-three-phase PMSM proposed in literature [5] in which two basic voltage vector is synthesized into a new intermediate vector, and a two-step model prediction is added to the traditional MPC algorithm. Two synthesized voltage vectors are selected in one cycle. This method can suppress the magnitude of the CMV, but the current tracking accuracy is low, and the stator current harmonics are not effectively suppressed.

For this reason, this paper takes the dual Y-shift  $30^\circ$  dual three-phase PMSM system with the star node of the stator winding as the research object, analyzes its mathematical model and the characteristics of the six-phase spatial common-mode voltage, and proposes a suppression of common-mode voltage characteristics. In the MPC current control (MPCC), by synthesizing the low CMV vector and introducing the duty cycle control, the optimal configuration of the action time of vector is realized. Under the condition that the stator harmonic current suppression effect is maintained, the CMV suppression is realized. And further simulation to verify the correctness and effectiveness of the method.

## 2 Dual-Three Phase PMSM Model and Common Mode Voltage Analysis

### 2.1 Dual-Three Phase PMSM Model Analysis

Figure 1 shows a system composed of a dual Y-shifted  $30^\circ$  dual three-phase PMSM designed with two sets of Y-connected windings phase shifted by  $30$  electrical degrees and a two-level voltage converter the stator.

The star junctions of the ABC winding, and the DEF winding are isolated, so in a balanced state it will not provide a loop for the 3rd harmonic current, and it is also isolated from the midpoint  $g$  of the DC bus of the converter.

If the voltage-type converter adopts the complementary working mode, the six-phase converter in Fig. 1 has 64 switch states. According to the vector space decoupling theory

(VSD), the basic voltage vector corresponding to the 64 switch states can be mapped to three mutually perpendicular planes through the coordinate transformation matrix, namely  $\alpha\beta$  plane,  $o1o2$  plane and  $z1z2$  plane as shown in Fig. 2.

The vector number in Fig. 2 is represented by an octal number and the order is ABCDEF. The binary number corresponding to the octal number represents the switching state of the 6 bridge arms in which 1 represents the upper bridge arm is turned on, and 0 represents the lower bridge arm is turned on.

According to the magnitude of the voltage amplitude in the plane, the voltage vector can be divided into 4 groups: Large ( $V_{max}$ ,  $0.644U_{dc}$ ), Mid Large ( $V_{midl}$ ,  $0.741U_{dc}$ ), Mid min ( $V_{mids}$ ,  $0.333U_{dc}$ ), Min ( $V_{min}$ ,  $0.173U_{dc}$ ).

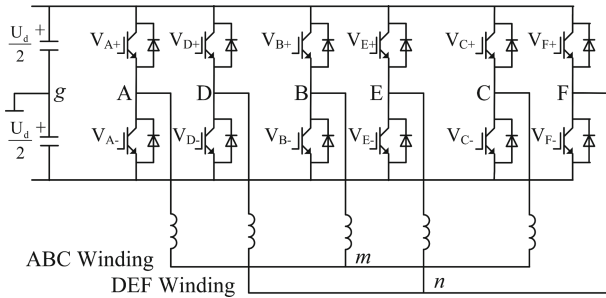


Fig. 1. System composed of dual Y shift 30° six-phase PMSM and converter

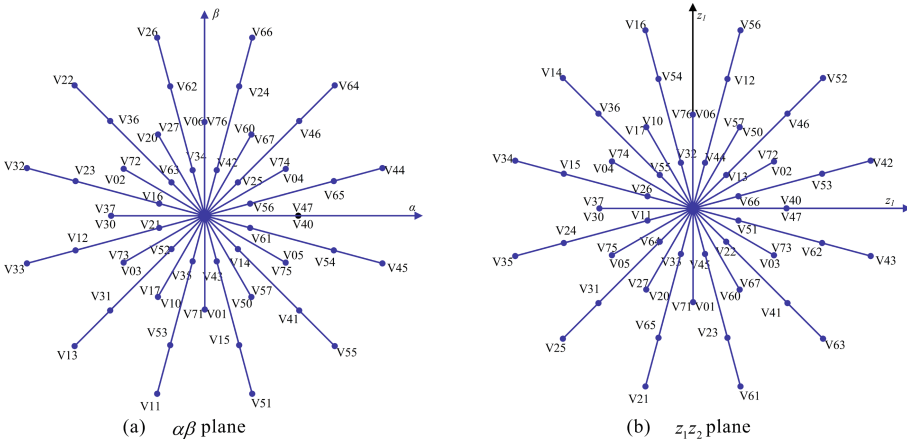


Fig. 2. 64 basic voltage vectors in  $\alpha\beta$  and  $z_1z_2$  planes

To simplify the analysis, the static coordinate system is converted into a synchronous rotating coordinate system, and the voltage equation of the  $dq$  plane is obtained as

$$\begin{cases} u_d = Ri_d + L_d \frac{di_d}{dt} - \omega_e L_q i_q \\ u_q = Ri_q + L_q \frac{di_q}{dt} + \omega_e L_d i_d + \omega_e \psi_f \end{cases} \quad (1)$$

$$\begin{cases} u_x = Ri_x + L_z \frac{di_y}{dt} \\ u_y = Ri_y + L_z \frac{di_x}{dt} \end{cases} \quad (2)$$

where  $u_d$ ,  $u_q$ ,  $u_x$  and  $u_y$  represent the stator voltages of the  $dq$  and  $xy$  subspaces;  $i_d$ ,  $i_q$ ,  $i_x$  and  $i_y$  represent the stator currents of the  $dq$  and  $xy$  subspaces;  $L_d$  and  $L_q$  represent the inductance in the  $dq$  coordinate system;  $L_z$  represent the leakage inductance;  $\omega_e$  represent the electrical angular velocity.

## 2.2 Dual-Three Phase PMSM CMV Analysis

The voltage  $u_{mg}$  and  $u_{ng}$  in Fig. 1 is the common-mode voltage of dual-three phase PMSM. The magnitude of the two common-mode voltages can be calculated as follows:

$$\begin{cases} u_{mg} = \frac{1}{3}(u_{Ag} + u_{Bg} + u_{Cg}) \\ u_{ng} = \frac{1}{3}(u_{Dg} + u_{Eg} + u_{Fg}) \end{cases} \quad (3)$$

According to (3), the magnitude of the two common-mode voltages generated by the 64 basic vectors can be calculated, as shown in Table 1.

It can be seen from Table 1 that the CMV peak values generated by the four zero vectors are the largest, all of which are  $U_{dc}/2$ . From the perspective of suppressing CMV, these four zero vectors should be avoided as much as possible. Define (4), (6), (8), (9)

**Table 1.** CMV values of 64 basic voltage vectors

Group	Basic voltage vector	$u_{mg}$	$u_{ng}$
(1)	00	$-U_{dc}/2$	$-U_{dv}/2$
(2)	01, 02, 04	$-U_{dc}/2$	$-U_{dc}/2$
(3)	10, 20, 40	$-U_{dc}/6$	$-U_{dc}/6$
(4)	11, 12, 14, 21, 22, 24, 41, 42, 44	$-U_{dc}/6$	$-U_{dc}/6$
(5)	03, 05, 06	$-U_{dc}/2$	$-U_{dc}/2$
(6)	13, 15, 16, 23, 25, 26, 43, 45, 46	$-U_{dc}/6$	$-U_{dc}/6$
(7)	30, 50, 60	$U_{dc}/6$	$U_{dc}/6$
(8)	31, 32, 34, 51, 52, 54, 61, 62, 64	$U_{dc}/6$	$U_{dc}/6$
(9)	33, 35, 36, 53, 55, 56, 63, 65, 66	$U_{dc}/6$	$U_{dc}/6$
(10)	07	$-U_{dc}/2$	$-U_{dc}/2$
(11)	17, 27, 47	$-U_{dc}/6$	$-U_{dc}/6$
(12)	37, 57, 67	$U_{dc}/6$	$U_{dc}/6$
(13)	70	$U_{dc}/2$	$U_{dc}/2$
(14)	71, 72, 74	$U_{dc}/2$	$U_{dc}/2$
(15)	73, 75, 76	$U_{dc}/2$	$U_{dc}/2$
(16)	77	$U_{dc}/2$	$U_{dc}/2$

as the small CMV group ( $G_S$ ), whose CMV peak value is only  $U_{dc}/6$ ; the zero vector group as the large CMV group ( $G_L$ ); the rest are medium common mode voltage group ( $G_M$ ).

### 3 MPC Strategy of CMV Suppression

In the FCS-MPC, when the sampling period is small enough, the forward Euler method is usually used to achieve discrete equation [7]. The predicted current value after decoupling transformation is

$$\begin{cases} i_d^{k+1} = \frac{T_s}{L_d} u_d^k + (1 - \frac{T_s R}{L_d}) i_d^k + T_s \omega_e \frac{L_q}{L_d} i_q^k \\ i_q^{k+1} = \frac{T_s}{L_q} u_q^k + (1 - \frac{T_s R}{L_q}) i_q^k - T_s \omega_e \frac{L_d}{L_q} i_d^k - \frac{T_s}{L_q} \omega_e \psi_f \end{cases} \quad (4)$$

where  $T_s$  represent the sampling period of system.

To compensate for the one-step delay in the MPC algorithm, this article uses MPC with delay compensation. The prediction value of current at time  $k + 2$  is

$$\begin{cases} i_q^{k+2} = \frac{T_s}{L_q} u_q^k + (1 - \frac{T_s R}{L_q}) i_q^{k+1} - T_s \omega_e \frac{L_d}{L_q} i_d^{k+1} - \frac{T_s}{L_q} \omega_e \psi_f \\ i_d^{k+2} = \frac{T_s}{L_d} u_d^k + (1 - \frac{T_s R}{L_d}) i_d^{k+1} + T_s \omega_e \frac{L_q}{L_d} i_q^{k+1} \end{cases} \quad (5)$$

Using the finite control set model forecasting method, the cost function is usually defined as

$$G = |i_d^* - i_d^{k+2}|^2 + |i_q^* - i_q^{k+2}|^2 + \lambda_{xy} (|i_x^* - i_x^{k+2}|^2 + |i_y^* - i_y^{k+2}|^2) \quad (6)$$

where \* represent the reference value,  $\lambda_{xy}$  represent the weighting factor of harmonic current component of  $xy$  plane.

When using conventional MPC methods to achieve CMV suppression of six-phase motors, CMV component can be added to the cost function to avoid the use of  $G_m$  and  $G_L$ .

$$\begin{aligned} G = & |i_d^* - i_d^{k+2}|^2 + |i_q^* - i_q^{k+2}|^2 + \lambda_{xy} (|i_x^* - i_x^{k+2}|^2 + |i_y^* - i_y^{k+2}|^2) \\ & + \lambda_L \cdot (V_i \in G_L) + \lambda_M \cdot (V_i \in G_M) \end{aligned} \quad (7)$$

where  $\lambda_L$  and  $\lambda_M$  represent the weighting factor;  $V_i \in G_L$  and  $V_i \in G_M$  are the logic function, if voltage vector is in group  $G_L$ ,  $G_M$ , its value is 1, otherwise 0.

The cost function has 3 weighting factors, which increases the difficulty and computational burden of adjusting the weighting factors and increases the complexity of the prediction model [8].

## 4 CMV Suppression of MPC with Virtual Vector

### 4.1 The Construction of Virtual Vector

Compared with the three-phase motor of the same capacity, the dual three-phase PMSM has relatively smaller stator winding impedance, which results in relatively large stator

harmonic currents. Therefore, it is also necessary to consider how to effectively suppress stator harmonic currents in the MPC method [6]. The two star-shaped nodes of the stator winding are isolated, which can make the harmonic current on the  $o_1o_2$  plane zero, but there are still harmonic currents on the  $z_1z_2$  plane.

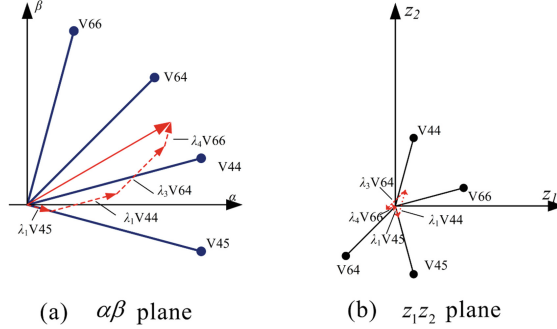


**Fig. 3.** The schematic diagram of  $V^3s$  construction

This article selects the adjacent largest four vectors to synthesize the  $V^3s$ , as shown in Fig. 3. The maximum voltage vector is in the  $G_L$  and  $G_M$ , which has the maximum magnitude on the  $\alpha\beta$  plane, while corresponding to the minimum magnitude on the  $z_1z_2$  plane.

To make the composite voltage of the  $z_1z_2$  plane is zero, we can make each vector work with a different duty cycle time. Therefore, the harmonic current in the plane  $z_1z_2$  can be effectively suppressed, and the action time of each vector can be obtained by the following

$$\begin{cases} 0.173V_{dc}(\lambda_1 \cos(-\frac{5\pi}{12}) + \lambda_2 \cos(\frac{5\pi}{12}) + \lambda_3 \cos(-\frac{3\pi}{4}) + \lambda_4 \cos(\frac{\pi}{12})) = 0 \\ 0.173V_{dc}(\lambda_1 \sin(-\frac{5\pi}{12}) + \lambda_2 \sin(\frac{5\pi}{12}) + \lambda_3 \sin(-\frac{3\pi}{4}) + \lambda_4 \sin(\frac{\pi}{12})) = 0 \end{cases} \quad (8)$$

where  $\lambda_1, \lambda_2, \lambda_3$  and  $\lambda_4$  represent the duty cycle of four vectors respectively. Assuming  $\lambda_2 = \lambda_3$ , it is possible to reach each duty cycle as

$$\begin{cases} \lambda_1 = 0.134 \\ \lambda_2 = 0.366 \\ \lambda_3 = 0.366 \\ \lambda_4 = 0.134 \end{cases} \quad (9)$$

The amplitude of the resultant voltage vector on the plane is

$$\begin{aligned} |\mathbf{V}_{v1}|_{\alpha\beta} &= 0.644V_{dc} \cos \frac{\pi}{12} (\lambda_2 + \lambda_3) \\ &+ 0.644V_{dc} \cos \frac{\pi}{4} (\lambda_1 + \lambda_4) \end{aligned} \quad (10)$$

Substituting (9) into (10), we get

$$|\mathbf{V}_{v1}|_{\alpha\beta} = 0.5774V_{dc} \quad (11)$$

In this way, the total  $V^3s$  combination is obtained, as shown in Fig. 4. The blue dot in the figure represents the maximum voltage vector, and the red dot represents the  $V^3s$ .

### 4.2 Simplified Cost Function and Prediction Model

The cost function is to select the optimal voltage vector in the MPC optimization process to achieve the best tracking performance [7]. For the control of dual three-phase PMSM, to reduce the harmonic current as much as possible, the reference value of  $i_x$  and  $i_y$  is usually set to 0. At the same time, the CMV component is added to the cost function, as in (7), which greatly increases the complexity of the cost function.

Through the  $V^3s$  method, the composite voltage of the  $z_1z_2$  plane is zero, and  $V^3s$  are all synthesized by the voltage vector with the smallest common-mode voltage. Therefore, the cost function is simplified, and this method reduces the computational burden.

$$G = \left| i_d^* - i_d^{k+2} \right|^2 + \left| i_q^* - i_q^{k+2} \right|^2 \tag{12}$$

There is no  $i_x$  and  $i_y$  component in the cost function, which also means that there is no need to perform iterative calculation of harmonic current, during the sampling period.

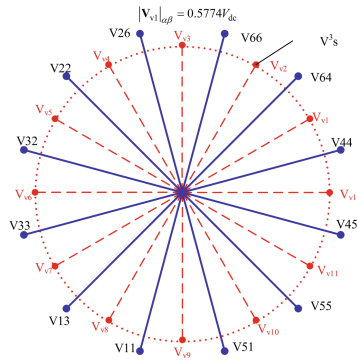


Fig. 4. Trajectories of  $V^3s$  and the large voltage vectors in  $\alpha\beta$  subspace

### 4.3 Estimation of Duty Cycle of $V^3s$

Generally, in a sampling period, the optimal  $V^3s$  does not need to be applied to the entire period to make the actual current follow the given value. Therefore, a zero-voltage vector can be introduced based on the traditional model to predict the current for duty cycle control, a  $V^3s$  is selected in each control period, and its optimal action time is calculated, and the remaining time is filled with a zero-voltage vector. The optimal duty cycle is to reduce the tracking error value, thereby reducing current ripple and improving the steady-state performance of the system [9].

In the MPC current prediction, assuming that the  $V^3$ s action time is  $dT_s$ , where  $d$  is the duty cycle, then the current at the beginning of the  $k + 2$  sampling period can be calculated as

$$\begin{cases} i_d^{k+2} = \frac{dT_s}{L_d} u_d^k + (1 - \frac{T_s R}{L_d}) i_d^{k+1} + T_s \omega_e \frac{L_q}{L_d} i_q^{k+1} \\ i_q^{k+2} = \frac{dT_s}{L_q} u_q^k + (1 - \frac{T_s R}{L_q}) i_q^{k+1} - T_s \omega_e \frac{L_d}{L_q} i_d^{k+1} - \frac{T_s}{L_q} \omega_e \psi_f \end{cases} \quad (13)$$

Obtain the duty cycle  $d$  when the cost function is minimized as

$$\frac{\partial G}{\partial d} = 0 \quad (14)$$

$$d = \frac{[i_d^* - (1 - \frac{RT_s}{L_d} i_d^{k+1}) - T_s \omega_e \frac{L_q}{L_d} i_q^{k+1}] V_d + [i_q^* - (1 - \frac{RT_s}{L_q} i_q^{k+1}) + T_s \omega_e \frac{L_d}{L_q} i_d^{k+1} + \frac{T_s}{L_q} \omega_e \psi_f] V_q}{(\frac{T_s}{L_d} V_d^2 + \frac{T_s}{L_q} V_q^2)} \quad (15)$$

where  $V_d$  and  $V_q$  are the components of the  $V^3$ s on  $d$  axis and  $q$  axis respectively;  $0 \leq d \leq 1$ .

#### 4.4 Vector Sequence Design

Generally, in the duty cycle MPCC, the optimal voltage vector acts for the time, and the zero-voltage vector fills the rest of the time [9], as Fig. 5 show. In this arrangement sequence, both sets of windings have produced 4 kinds of CMV. Among them, when the zero-voltage vector is applied, the CMV peak value of the two sets of windings has reached  $V_{dc}/2$ .

To reduce the CMV, this paper chooses two voltage vectors with opposite phases to replace the zero-voltage vector, and the order of the vector action is asymmetrical. In this combination scheme, the order of action of the maximum basic voltage vector can be counterclockwise or clockwise. To reduce the extra switching action, the clockwise and counterclockwise order of action can be substituted for each other.

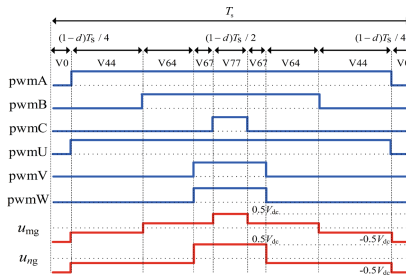
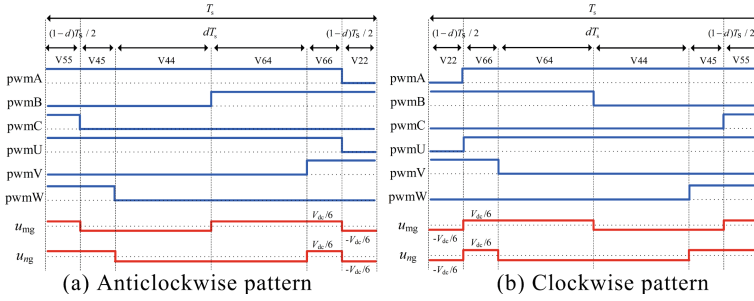


Fig. 5. Conventional switching pattern

When  $Vv1$  or  $Vv7$  is the optimal virtual voltage vector, two voltage vectors with opposite phases,  $V55$  and  $V22$ , are selected to replace the zero-voltage vector, and the volt-second value of each control cycle is adjusted. The six voltage vector combinations that replace the zero vector are shown in Table 2. The selection of the combination is determined by the optimal virtual voltage vector.





**Fig. 6.** Asymmetrical switching patterns

**Table 2.** Phase opposed vectors in Asymmetrical patterns

Optimal virtual voltage vector $V_{opt}$	Composite zero vector combination
$V_{v1}, V_{v7}$	$0.5V_{55} + 0.5V_{22}$
$V_{v2}, V_{v8}$	$0.5V_{45} + 0.5V_{32}$
$V_{v3}, V_{v9}$	$0.5V_{44} + 0.5V_{33}$
$V_{v4}, V_{v10}$	$0.5V_{64} + 0.5V_{13}$
$V_{v5}, V_{v11}$	$0.5V_{66} + 0.5V_{11}$
$V_{v6}, V_{v12}$	$0.5V_{26} + 0.5V_{51}$

### 4.5 Proposed SCMV-MPCC Method

Based on the  $V^3$ s and asymmetrically optimized switching sequence, this paper proposes an improved dual three-phase permanent magnet synchronous motor model predictive current control method.

This method simplifies the cost function, the prediction model delays the compensation link, and only performs 12 calculations in each control cycle, which reduces the calculation burden. Adding duty cycle estimation before current prediction improves the tracking accuracy of the system. The flow chart of the improved dual three-phase permanent magnet synchronous motor model predictive current control method is shown in Fig. 7.

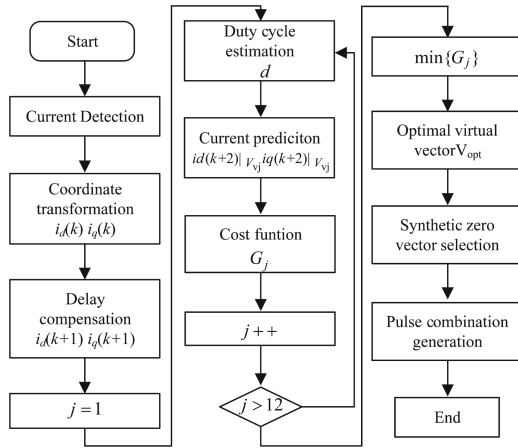


Fig. 7. Flowchart of the proposed SCMV-MPCC method

### 5 Simulation

To verify the correctness and effectiveness of the method proposed in this paper, a simulation model of a two-level inverter driving a dual-Y shifted 30° dual three-phase PMSM system is established in the MATLAB/Simulink environment. The DC bus voltage of the inverter in the simulation model is 570 V, and the motor parameters are shown in Table 3.

Table 3. The parameters of dual three-phase PMSM

Parameter	Value
Poles pairs	5
d axis inductance $L_d$ (mH)	27.5
q axis inductance $L_q$ (mH)	48.3
Stator leakage inductance $L_{1s}$ (mH)	24.5
Stator resistance $R$ ( $\Omega$ )	1.8856
Rotor flux $\Psi_f$ (Wb)	1.192
Inertia $J$ ( $\text{kg}\cdot\text{m}^2$ )	0.01
Rated torque $T_N$ (N·m)	150
Rated speed $n_N$ ( $\text{r}\cdot\text{min}^{-1}$ )	300

The control period is 0.0001 s. According to the above parameters, the MPCC without CMV suppression [10, 11] and the  $V^3$ s optimized MPC current control with CMV suppression are simulated. The steady-state ABC winding MCV waveform, stator A-phase current waveform, and steady-state fast FFT analysis of these two methods are

shown in Fig. 8 and 9. Figure 8 (a) and (b) are the CMV waveforms of the two methods respectively. The positive peak value of the CMV of the two methods is 95 V, the negative peak value without CMV suppression is  $-285$  V, and the peak-to-peak value is 380 V; the negative peak value with CMV suppression is  $-95$  V, the peak-to-peak value is 190 V. The magnitude of the voltage has been effectively suppressed. Figure 9 is a FFT analysis of the stator A-phase current waveform in 0.6–0.84 s. The results show that the stator A-phase current of the two methods in the steady state are both 25 Hz sine waves. The steady-state amplitudes are 8.479 A and 8.794 A, and the THD is 7.63% and 5.51% respectively. The THD of the SCMV-MPCC is slightly better than that of the MPCC without CMV suppression, because the voltage vector of the  $V^3$ s introduced by the former is synthesized to 0 in the  $z_1z_2$  plane. In the SCMV-MPCC, a low CMV zero vector is synthesized, and duty cycle control is introduced to realize the optimal configuration of the action time. The above simulation results show that compared with the MPC of dual three-phase PMSM without CMV suppression, the SCMV-MPCC can effectively suppress the magnitude of CMV and effectively suppress stator harmonic currents.

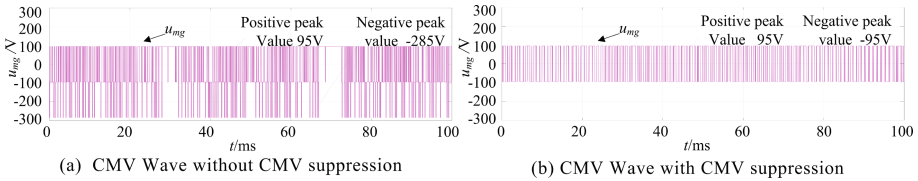


Fig. 8. CMV simulation waveform of ABC winding

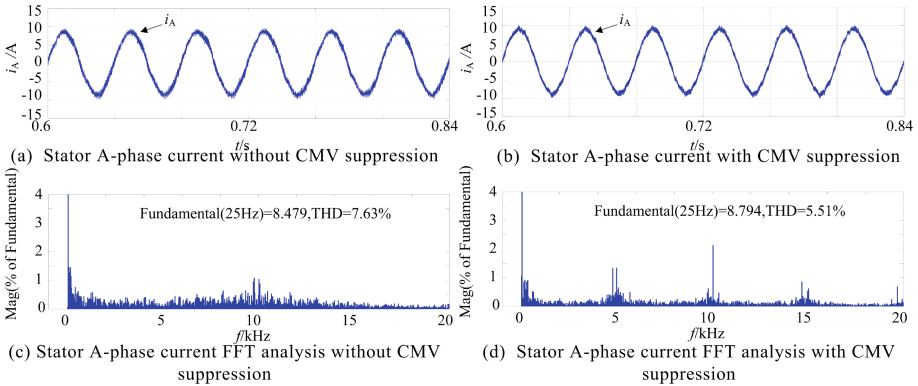


Fig. 9. Current waveform of stator A-phase and its steady-state FFT analysis

## 6 Conclusion

In this paper, a system composed of a double Y-shifted  $30^\circ$  dual three-phase PMSM and a two-level voltage-type converter, which is isolated from the star node of the stator

winding, is used to analyze the CMV characteristics of the six-phase voltage space. A SCMV-MPCC method is proposed that selects the largest adjacent four vectors among 64 basic vectors to synthesize the effective  $V^3$ s that can suppress the CMV. The  $V^3$ s is a zero vector in the  $z_1z_2$  plane to suppress the stator harmonic current, thereby ignoring the CMV component and the  $z_1z_2$  plane harmonic current component in the cost function, avoiding multi-weight factor adjustment, and optimizing the prediction model.

The SCMV-MPCC method introduced duty cycle control by synthesizing a low CMV zero vector, to optimize the configuration of the  $Vs^3$  and the synthesized zero vector and reduce current ripple. The simulation results show that the proposed SCMV-MPCC can effectively suppress the common mode voltage while keeping the stator harmonic current suppression effect good.

**Acknowledgment.** This work was supported in part by the National Natural Science Foundation of China under Grant (52107045), in part by the Hunan Provincial Natural Science Foundation of China under Grant (2021JJ40078), in part by the National Natural Science Foundation of China under Grant (51737004) and in part by the Postgraduate Scientific Research Innovation Project of Hunan Province under Grant (QL20210099).

## References

1. Zhang, Z., Wu, X., Liu, X.: Low common mode interference SVPWM control for dual three phase permanent magnet synchronous motor. *Trans. China Electrotech. Soc.* **33**(S1), 58–66 (2018). (in Chinese)
2. Ma, X., Ren, X., Yan, B.: Strategy of reducing the common mode voltage modulation of a three-level matrix converter. *Power Syst. Prot. Control* **48**(21), 49–57 (2020). (in Chinese)
3. Zhang, J., Gao, Z., Dong, Q.: Research on suppression of photovoltaic DC side common-mode voltage interference. *Power Syst. Prot. Control* **47**(14), 102–108 (2019). (in Chinese)
4. Cao, C., Lan, Z., Shen, F.: Review of initial position angle detection in sensorless control system of permanent magnet synchronous motor. *Electr. Eng.* **21**(06), 1–6 (2020). (in Chinese)
5. Zhang, Z., Wu, Y., Ye, S.: Model predictive control method with common-mode voltage suppression for dual three-phase permanent magnet synchronous motor. *Int. J. Appl. Electromagn. Mech.* **64**, 1453–1460 (2020)
6. Zheng, J., Rong, F., Huang, S.: Dual Y shift  $30^\circ$  six-phase SVPWM method based on suppression of common-mode voltage. *Proc. CSEE* **37**(24), 7338–7349+7448 (2017). (in Chinese)
7. Yu, B., Song, W., Li, J.: Improved finite control set model predictive current control for five-phase VSIs. *IEEE Trans. Power Electron.* **36**(6), 7038–7048 (2020)
8. Shen, Z., Jiang, D., Liu, Z.: Common-mode voltage elimination for dual two-level inverter-fed asymmetrical six-phase PMSM. *IEEE Trans. Power Electron.* **35**(4), 3828–3840 (2019)
9. Alcaide, A., Wang, X., Yan, H.: Common-mode voltage mitigation of dual three-phase voltage source inverters in a motor drive application. *IEEE Access* **9**, 67477–67487 (2021)
10. Guo, L., Jin, N., Li, Y.: Virtual vector based model predictive common-mode voltage reduction method for voltage source inverters. *Trans. China Electrotech. Soc.* **35**(04), 839–849 (2020). (in Chinese)
11. Guo, L., Jin, N., Shen, Y.: A mode predictive common-mode voltage suppression method for voltage source inverter based on optimum voltage vector selection. *Trans. China Electrotech. Soc.* **35**(04), 839–849 (2020). (in Chinese)